ACS APPLIED MATERIALS & INTERFACES

Research Article

www.acsami.org

Rare Earth-Modified Kaolin/NaY-Supported Pd–Pt Bimetallic Catalyst for the Catalytic Combustion of Benzene

Shufeng Zuo,*[,†] Xuejie Sun,[‡] Ningning Lv,[†] and Chenze Qi*[,†]

[†]Zhejiang Key Laboratory of Alternative Technologies for Fine Chemicals Process Shaoxing University, Shaoxing University, Shaoxing 312000, P. R. China

[‡]Esteve Huayi Pharmaceutical Co., Ltd., Shaoxing 312000, P. R. China

ABSTRACT: A new type of porous kaolin/NaY composite (KL-NY) with a large specific surface area and large pore sizes was synthesized through a one-step crystallization process, and rare earth-modified KL-NY-supported Pd–Pt catalysts were studied for benzene combustion. The results indicated that the pore volume and specific surface area of KL-NY after calcination and crystallization were 0.298 cm^3/g and 365 m^2/g, respectively, exhibiting appropriate pore structure and good thermal stability. Catalysts with rare earth metals greatly enhanced the activity of Pd/KL-NY, and the addition of Pt and Ce into the Pd catalyst improved the catalytic activity as well as the stability. The catalyst with an optimal Ce content and Pt/Pd molar ratio (0.2%Pd–Pt (6:1)/6%Ce/KL-NY) demonstrated the best activity for the complete oxidation of benzene at 230 °C, and the catalyst above maintained the 100% benzene conversion for 960 h.

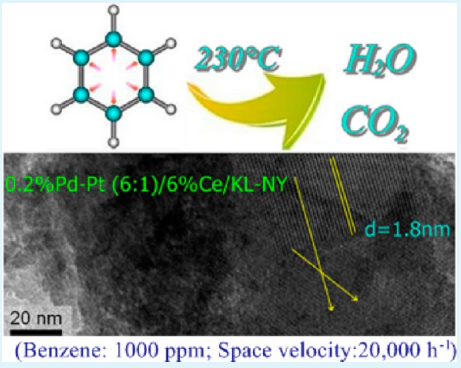

KEYWORDS: *kaolin/NaY, rare earth, Pd–Pt, volatile organic compounds, catalytic combustion*

INTRODUCTION

Volatile organic compounds (VOCs) are widely in use in various industrial areas, but they are not environmentally friendly because of their malodorous nature and toxicity. Therefore, appropriate control of VOCs is necessary, and furthermore, reduction and removal are crucial for environmental protection.[1,2] The best available techniques for reducing VOC emissions include adsorption, filtration, thermal and catalytic oxidation,[3] among which catalytic oxidation indicates the best effectiveness for low concentrations of VOCs.[4,5]

For catalytic oxidation, catalyst selection is the most important factor. Precious metal and transition metal oxide catalysts have been broadly explored for halogenated and non-halogenated compounds.[6−9] In spite of their high cost, noble metal-based catalysts maintain the advantage of high specific activity, stability, and ability to be regenerated.[10] The catalytic activity of noble metals strongly depends on the preparation method, type of precursor, metal loading, and particle size, as well as the nature of the support.[11−16] In particular, platinum and palladium are the two metal catalysts that have been effectively used,[17−19] and on the other hand, combinational catalysts, especially those based on Pt and Pd, have been studied in many researches.[20] By adding Pt metal in Pd catalysts, the catalytic activity can be significantly improved. Bimetallic systems are an interesting alternative to improve the catalyst property and/or have synergistic effects such as electronic effect/geometry effects. Although the scientific rationale is not clear yet, bimetallic systems improve both the selectivity and activity for a significant amount of reactions.[21,22]

Rare earth metals, especially Ce and La, are interesting materials for promoter and reducible support. Their unique ability for storing and releasing oxygen makes them attractive catalysts as they can provide lattice oxygen, and if incorporated with noble metal, the sintering of noble metal can be avoided.[23,24] This characteristic improves the dispersion of supported metals, the thermal resistance of the supports, the oxidation and reduction of supported noble metals, and prevents coke formation on the catalyst surface.[25−30] In recent years, a considerable amount of attention has been given to ceria-modified noble metal catalysts because of their application in the exhaust systems of automobiles. Ceria works as a promoter due to the unique redox characteristic and high oxygen storage capacity (OSC), as well as the stabilization of metal dispersion.[31,32]

Support is another important factor for Pd–Pt-loaded catalysts and can deeply affect the catalytic performance.[33,34] Various supports, such as porous materials, alumina, and silica, have been widely studied in the researches for hydrocarbon catalytic oxidation.[35−38]

Kaolin, a low-cost and economical raw material, has been used for the synthesis of various zeolites such as ZSM−5, NaY,[39,40] and Y-faujasite[41] as it contains the proper ratio of SiO_2 and Al_2O_3. Kaolin is an attractive adsorbent and catalyst support because its surface can be modified, enhancing the textural properties of the catalyst such as the pore volume and

Received: January 8, 2014
Accepted: July 24, 2014
Published: July 24, 2014

adjustable surface area.[42,43] To the best of our knowledge, the application of kaolin in the area of VOCs complete oxidation has not been reported yet. So our study could be of interest for those areas that can benefit from utilizing kaolin materials. In the present investigation, with kaolin as the starting material, a novel kaolin/NaY material (KL-NY) of micromesoporous structure was prepared by a one-step method. The addition of rare earth metals into KL-NY improved the thermal resistance for the supports and enhanced dispersion of the supported metals. So such a material with a rare earth promoter can work as an effective carrier for Pd−Pt catalyst in the catalytic oxidation of VOCs.

In the present study, KL-NY prepared by a one-step crystallization process was used as a support for rare earth metal and Pd−Pd oxides. The aim of the present study was to evaluate the stability and activity of the Pd catalysts with Ce and Pt. Rare earth metal and Pd−Pd oxides were introduced to KL-NY by incipient wetness impregnation. Characterization was performed by techniques of X-ray diffraction (XRD), N_2 adsorption/desorption, transmission electron microscopy (TEM), scanning electron microscopy (SEM), energy dispersive X-ray spectrometry (EDS), and H_2 temperature-programmed reduction (H_2-TPR).

EXPERIMENTAL DETAILS

Preparation of the Support and Catalyst. The preparation of solid kaolin/NaY composite (KL-NY) was detailed in the scientific literature by Liu, H.[44] REE/KL-NY (REE = Y, Ce, La, Pr, and Nd) was prepared by the similar impregnation method as explained in our previous research.[25] The REE content was 6 wt %. (The catalysts with 6−8 wt % REE loading indicated the best performance.)

KL-NY- and REE/KL-NY-supported Pd−Pt catalysts were obtained by impregnation with a 10 mg/mL aqueous solution of H_2PtCl_6 and H_2PdCl_4, while different catalysts were obtained by using different ratios of Pd/Pt during preparation. The impregnated samples were reduced, filtered, and then washed with sufficient quantity of deionized water until no chlorides were observed. Then the samples were dried at 110 °C and calcined at 400 °C for 2 h. The total contents of Pd and Pt for all the prepared catalysts were 0.2 wt %.

Characterization and Catalytic Tests. The samples were characterized by powder XRD for phase composition. The specific surface area (S_{BET}), total pore volume (V_p), micropore volume (V_{mic}), and mesopore area (A_{mes}) of the samples were determined by N_2 adsorption isotherms. Hydrogen chemisorptions were used to determine Pd dispersion. SEM-EDS and high-resolution (HR) TEM-EDS techniques were employed to observe the catalyst morphology and particle size. H_2-TPR measurements were performed to determine the reducibility of the catalysts. All the characterization methods for the supports and catalysts have been reported and detailed in our previous research.[9,25,45] The catalytic activity of catalysts was determined by benzene oxidation carried out in a microreactor, with the same methodology as previously reported by our research group.[45]

RESULTS AND DISCUSSION

XRD Analysis. In Figure 1, the samples exhibited strong reflections characteristic of $Na_2Al_2Si_4O_{12}\cdot 8H_2O$. No additional peaks related to ceria phases were detected for catalysts containing Ce, which indicated that the dispersion of ceria on KL-NY was high or that the peaks were overshadowed by those of KL-NY. Moreover, metallic peaks for Pt or Pd were not observed, showing that the PtO_2 or PdO particles were small, which is below the X-ray detection range. The results also showed that the Pt and Pd loading were low on the high surface

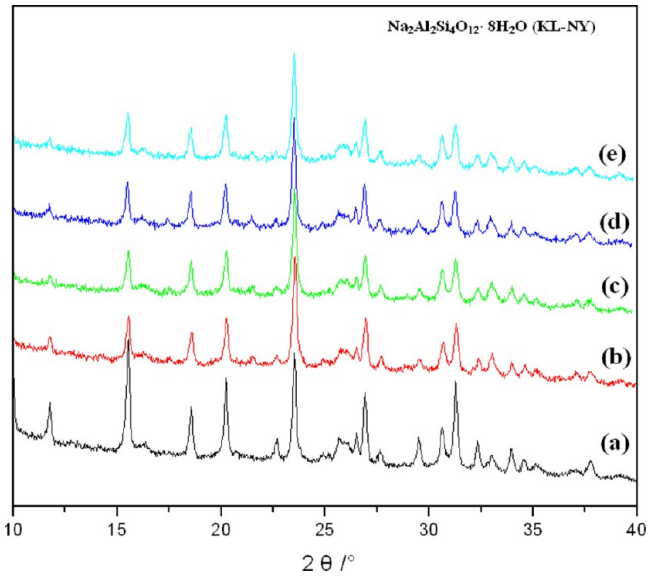

Figure 1. XRD graphics: (a) KL-NY; (b) Ce/KL-NY; (c) Pd/KL-NY; (d) Pd/Ce/KL-NY; (e) Pd−Pt (6:1)/Ce/KL-NY.

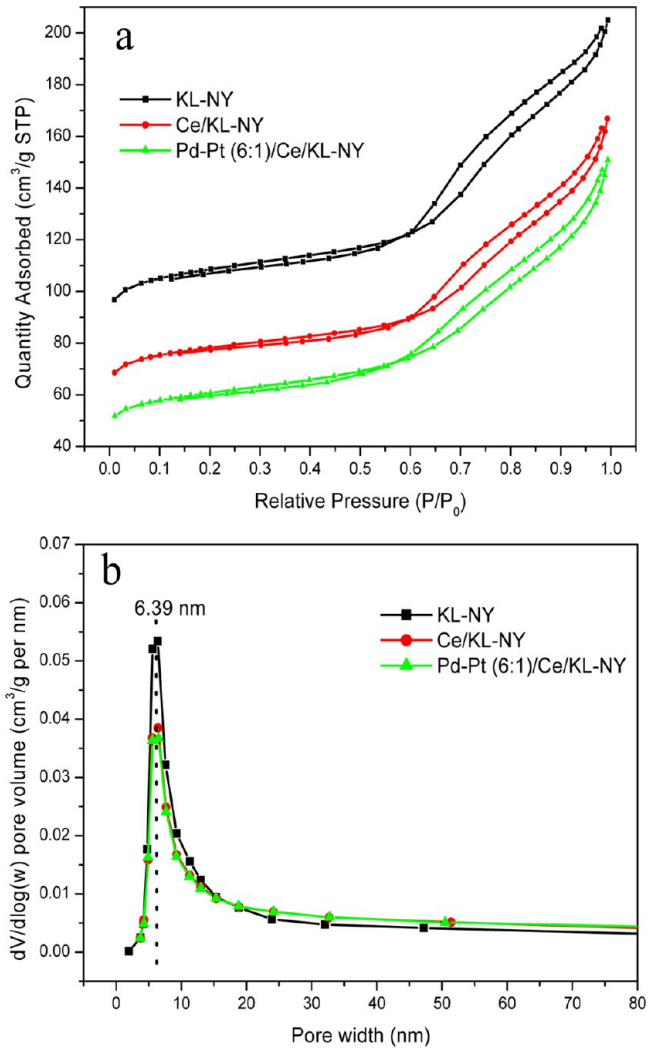

Figure 2. Characteristics of the samples. (a) N_2 adsorption/desorption isotherms. (b) Pore volume distribution.

Table 1. Characteristics of the Samples: Surface Area, Pore Volume, and Diameters of Pd Crystallites

samples	S_{BET}[a] (m^2/g)	A_{mes}[b] (m^2/g)	V_p[c] (cm^3/g)	V_{mic}[d] (cm^3/g)	catalysts	H/Pd[e]	d (nm)[f]
KL-NY	365	76	0.296	0.134	Pd/KL-NY	0.190	5.86
Ce/KL-NY	264	63	0.234	0.093	Pd/Ce/KL-NY	0.261	4.27
Pd−Pt (6:1)/Ce/KL-NY	241	61	0.222	0.084	Pd−Pt (6:1)/Ce/KL-NY		

[a]BET specific surface area. [b]Calculated from BJH method. [c]Total pore volume estimated at $P/P_0 = 0.99$. [d]Calculated from the t-plot method. [e]Molar ratio of adsorbed hydrogen atoms to the total palladium atoms. [f]Calculated diameters of palladium crystallites based on the dispersion of Pd.

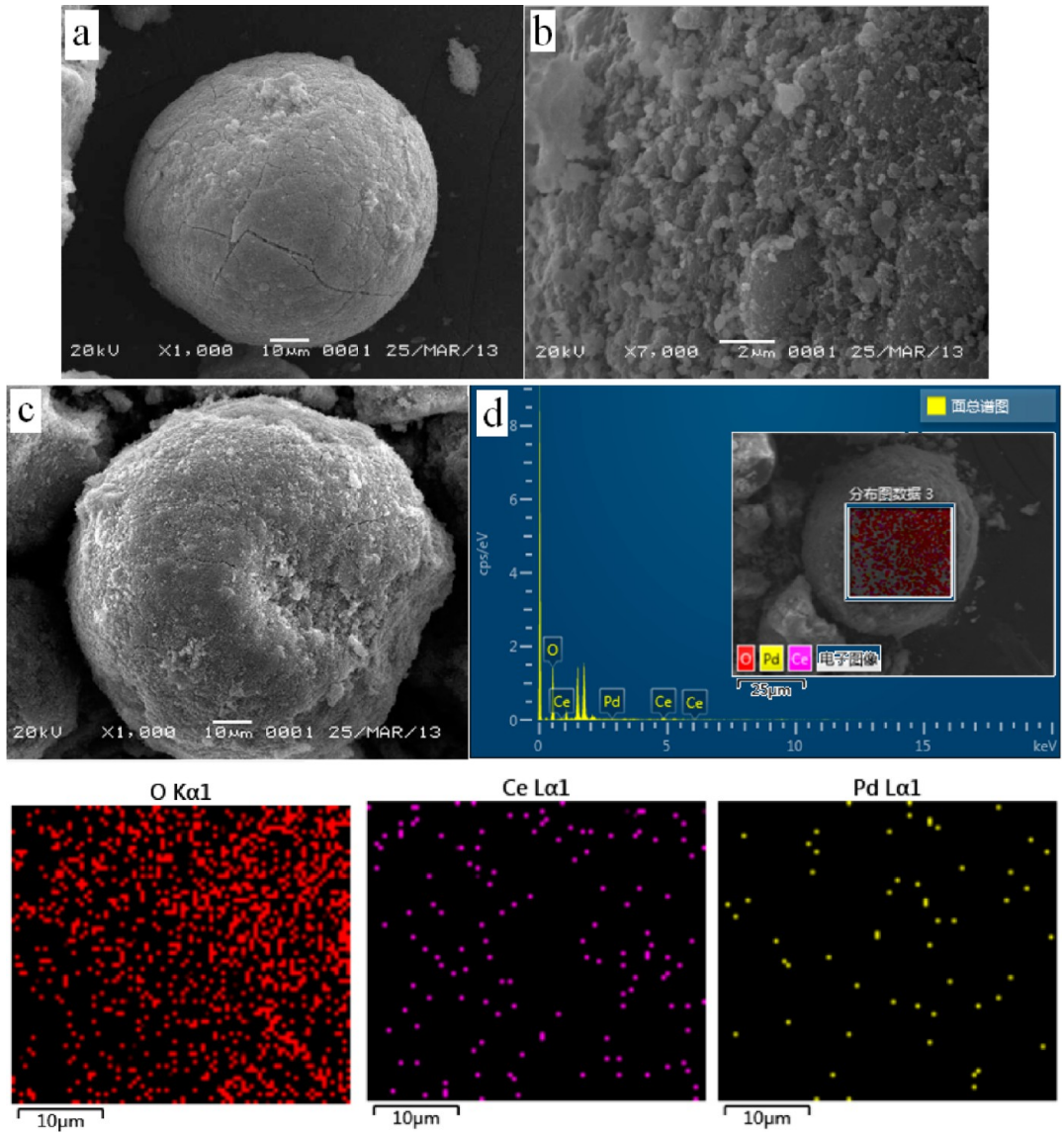

Figure 3. SEM images. (a) KL-NY surface microsphere. (b) The section of KL-NY microsphere. (c) The surface of Pd−Pt (6:1)/Ce/KL-NY microsphere. (d) EDS pattern of Pd−Pt (6:1)/Ce/KL-NY.

area supports, and the metals were highly dispersed. Consequently, no Pt and Pd peaks were detected.

N_2 Adsorption/Desorption and Pd Particle-Size Analysis. In Figure 2, all of the adsorption isotherms and hysteresis loops of the samples appeared to be of type VI, according to the Brunauer, Deming, Deming, and Teller classification,[46] indicating the presence of a characteristic pore structure with a parallel wall and a slit-shape. In all of the isotherms shown in Figure 2a, the desorption branch showed an inflection knee at 0.15 and 0.60 P/P_0, indicating framework-confined micro-mesoporous composite structure. The N_2 adsorption/desorption branches of the isotherms of the KL-NY support displayed a steeper fall and a larger hysteresis loop than the supported catalysts, indicating that large pores were present in the catalyst.

In Table 1, the S_{BET} for KL-NY was 365 m^2/g, and the corresponding V_p was 0.296 cm^3/g. After the addition of Ce and Pd−Pt, the S_{BET} and V_p decreased to 264 m^2/g and 0.234 cm^3/g for Ce/KL-NY and 241 m^2/g and 0.222 cm^3/g for Pd−Pt. Although the isotherms of the supported catalysts were somewhat different from that of KL-NY, mesopores were maintained, and the pore size distribution exhibited narrower

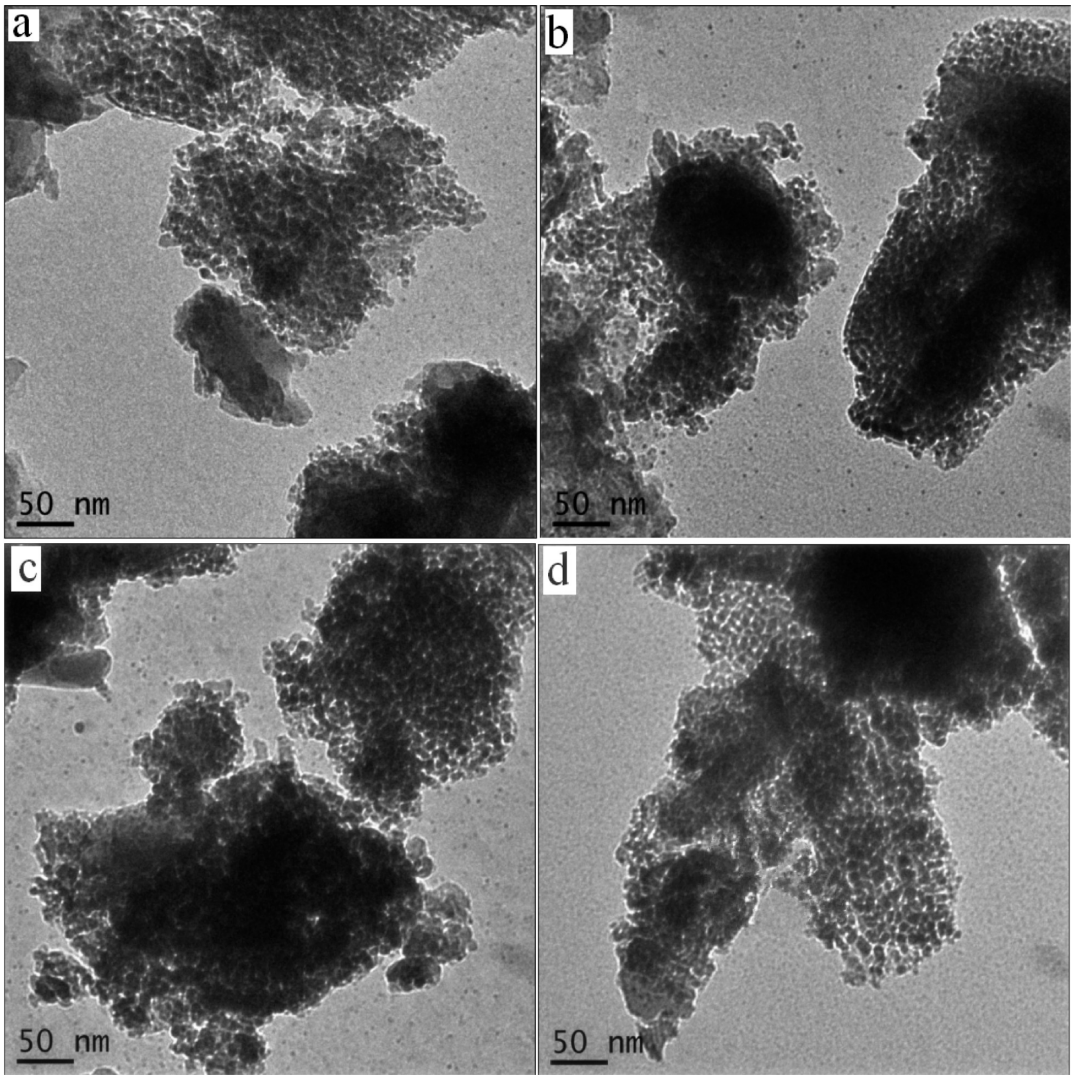

Figure 4. TEM images of KL-NY: (a) KL-NY; (b) Ce/KL-NY; (c) Pd/Ce/KL-NY; (d) Pd−Pt (6:1) /Ce/KL-NY.

half peak widths, centered at 6.39 nm, indicating the uniform mesopores of the synthesized catalysts (Figure 2b).

The addition of Ce and Pd−Pt into KL-NY decreased the N_2 adsorption capacity, which was indicative of a reduction in the $S_{BET,}$ A_{mes}, V_p, and V_{mic}. The pore volume decrease indicates that doped cations entered the micromesopores of KL-NY upon impregnation, forming CeO_2, PtO_2, and PdO in the pores and surface after calcination.

Table 1 shows the H/Pd ratio and calculated mean Pd particle size of various catalysts. The H/Pd ratio of Pd/Ce/KL-NY was higher than that of Pd/KL-NY. Thus, the dispersion of Pd was related to the addition of Ce. That is, the addition of Ce improved the dispersion of Pd. In the present study, we believe that the improved Pd dispersion and the high oxygen storage of Ce enhanced the catalytic activity of the catalysts.

SEM and TEM Analysis. The SEM images for KL-NY microspheres and the Pd−Pt(6:1)/Ce/KL-NY are shown in Figure 3. The section morphologies were examined by cutting out the microspheres to hemispheres. The section of the kaolin microspheres [Figure 3b] showed a disordered stack of particles. However, the surface of kaolin microspheres was smooth [Figure 3a], as it was covered by silica sol. Unlike the KL-NY, however, two phases were found on the Pd−Pt(6:1)/Ce/KL-NY, as shown in Figure 3c. The PdO, PtO_2, and CeO_2 particles gathered on the surface of microspheres, forming a smooth surface layer. To analyze the dispersion of the active phase on the support surface, Pt, Pd, and Ce mapping using SEM-EDS was made. In Figure 3d, the EDS images of Pd−Pt(6:1)/Ce/KL-NY showed the signals of Pd, Ce, and O, and no Pt signal was found because Pt loading was very low, demonstrating the active components had successfully loaded and were highly dispersed on the surface of KL-NY.

The TEM images of KL-NY and the supported catalysts are shown in Figure 4. For KL-NY, NaY crystals were densely packed on the surfaces of the kaolin. NaY crystals presented a typical mesoporous structure with uniform distribution, and the particle sizes were approximately 5−10 nm. After the addition of Ce and precious metals, the particle sizes of KL-NY did not change significantly, and the mesoporous system was successfully replicated by the metal oxide and presented an ordered framework.

The HRTEM image of the Pd−Pt(6:1)/Ce/KL-NY is shown in Figure 5. The layers were obviously kept apart with the highly ordered two-dimensional layered structure, obtaining large pore structures, and the basal spacing between two neighboring fringes was about 1.8 nm. On the surface of KL-NY, CeO_2 nanoparticles could be observed clearly and were dispersed randomly, and the detected CeO_2 particles sized in

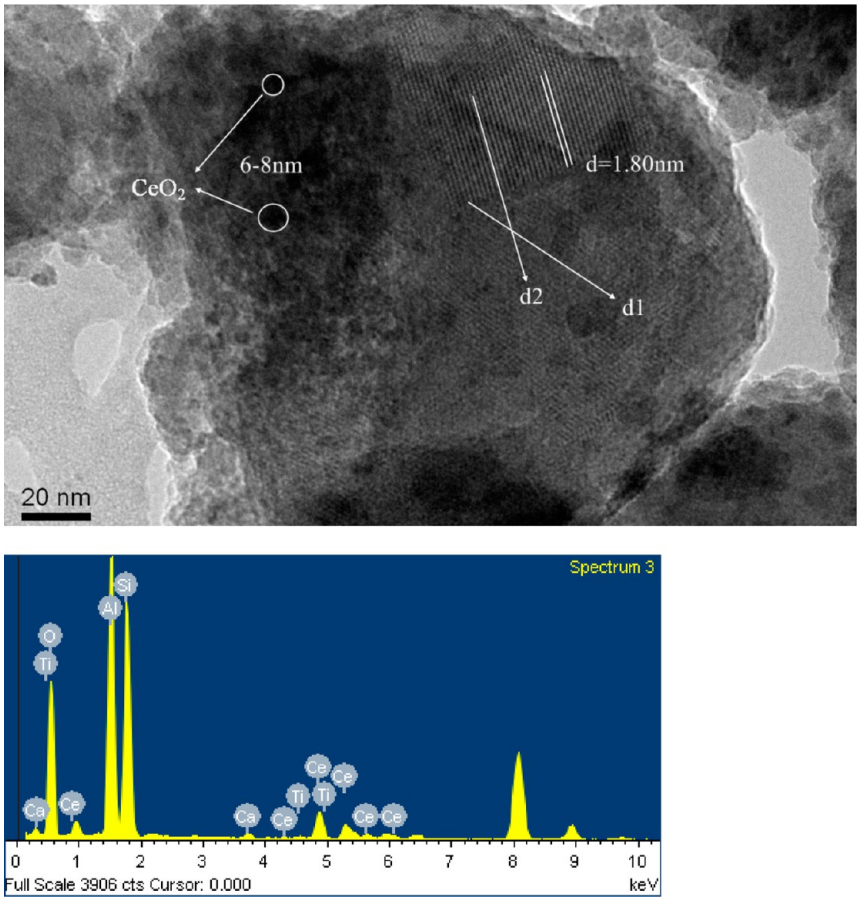

Figure 5. HRTEM image and EDS of Pd−Pt (6:1)/Ce/KL-NY.

the range of 6−8 nm. The EDS image of Pd−Pt(6:1)/Ce/KL-NY showed the signals of Ce, demonstrating the successful loading of CeO_2 on mesoporous KL-NY. However, no Pd and Pt signals were found.

Catalytic Activity and Stability Tests. The effects of REE addition on the catalytic activity of Pd/KL-NY for deep benzene oxidation are shown in Figure 6a. In the case of KL-NY and Ce/KL-NY, the conversions were very low, 60% and 85%, respectively, at a reaction temperature of 450 °C. The results indicated that by adding REE the catalytic activity of the Pd catalysts (excluding Nd) can be significantly improved, especially the ceria-modified Pd/KL-NY catalyst, which shows the best performance. The temperature for the complete conversion of benzene was approximately 270 °C. In ceria-based catalysts, reducible ceria may also supply adsorbed oxygen species, which can spill over from the support to the metal particles, and reduced Ce^{3+} can be reoxidized by oxygen:

$$2Ce^{4+} + O^{2-} + * \rightarrow 2Ce^{3+} + O*$$

$$2Ce^{3+} + 1/2O_2 \rightarrow 2Ce^{4+} + O^{2-}$$

* represents crystalline lattice.

Thus, during the reaction process, ceria could supply active oxygen species to the metal oxide, greatly improving the oxidation ability of PdO. The activity of the catalysts decreased according to the following order: Pd/Ce/KL-NY > Pd/La/KL-NY > Pd/Y/KL-NY > Pd/Pr/KL-NY > Pd/KL-NY, Pd/Nd/KL-NY. Because the ceria-modified Pd catalyst indicated the best activity, our research studied the effects of the second noble metal (Pt) on the catalytic activity of Pd/Ce/KL-NY in the benzene complete oxidation.

The effect of the Pd content (Pd/Pt = 1:3, 1:1, 3:1, 6:1, and 9:1) with approximately 0.2 wt % total metal loading on Pd−Pt/Ce/KL-NY catalysts was examined in the deep oxidation of benzene, as shown in Figure 6b. Pd−Pt bimetallic catalysts displayed better conversion than monometal catalysts. Pd−Pt bimetallic catalysts provided better conversion because of the synergetic effect of Pt and Pd metal. Pd−Pt (6:1) catalysts presented the greatest activity among Pd−Pt bimetallic catalysts, and the temperature of the complete conversion of benzene was approximately 230 °C. Although the activity of Pt is superior to that of Pd in the oxidation of benzene in this research, the activity of bimetallic catalysts with excess Pt decreased.

Compared with other reported Pd−Pt loaded catalysts,[47−51] our catalysts display great performance in benzene deep oxidation, as shown in Table 2. Generally, the temperatures are over 220 °C for 90% benzene conversion. Lambert et al.[50] reported Pd/SiO_2 catalyst study for benzene oxidation, and the temperature for 90% benzene conversion was ∼197 °C. However, the synthesis method for this catalyst is complicated, and the gas hourly space velocity (GHSV) (∼800 h^{-1}) was much lower than that in our research. Results from our research indicated that the KL-NY materials are very promising catalysts for benzene oxidation.

Figure 7 shows the time course of the catalytic activities of Pd/KL-NY, Pd/Ce/KL-NY, and Pd−Pt (6:1)/Ce/KL-NY in the complete oxidation of benzene at 320 °C for 960 h. In the beginning of the reaction, the activity of the Pd/KL-NY catalyst

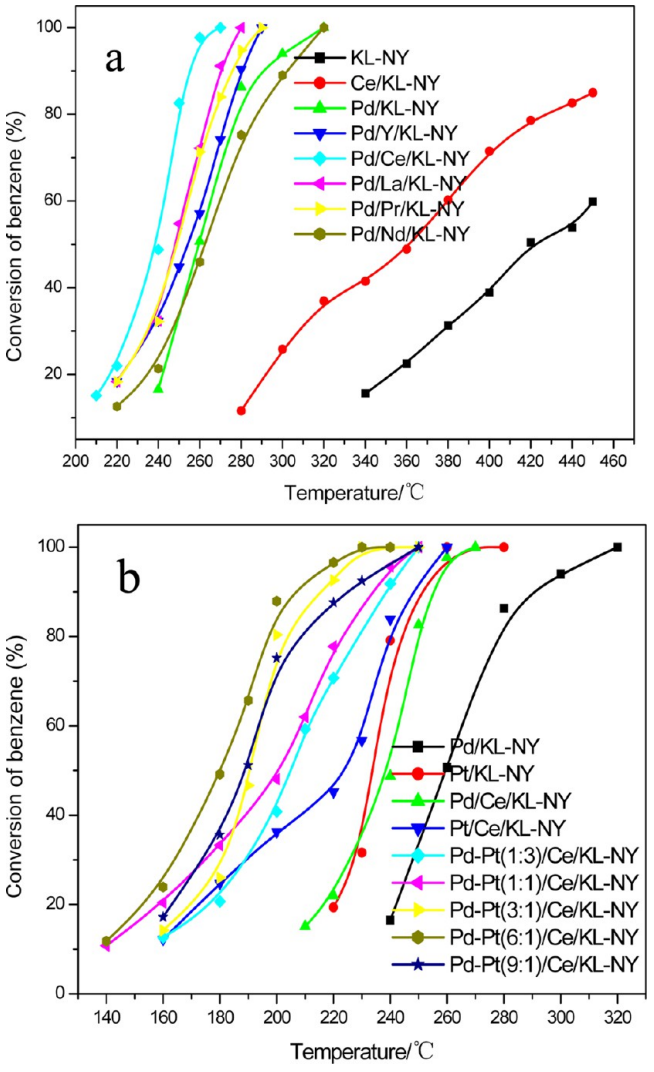

Figure 6. (a) Influence of the addition of rare earth into Pd/KL-NY for benzene complete oxidation. (b) Influence of the addition of Pt into Pd/Ce/KL-NY for benzene complete oxidation.

was similar to that of Pd/Ce/KL-NY and Pd−Pt (6:1)/Ce/KL-NY catalysts, but the activity decreased gradually over time. A slow decrease in the conversion was observed in the Pd/Ce/KL-NY catalyst after 480 h. However, the Pd−Pt (6:1)/Ce/KL-NY catalyst maintained the same high activity for 960 h. We confirmed that the addition of Pt and Ce to the Pd/KL-NY catalyst increased the catalytic activity and prevented catalyst deactivation.

H_2-TPR Analysis. Figure 8a displays the TPR profiles associated with Pd/KL-NY, Pd/Ce/KL-NY, and Pd−Pt(6:1)/

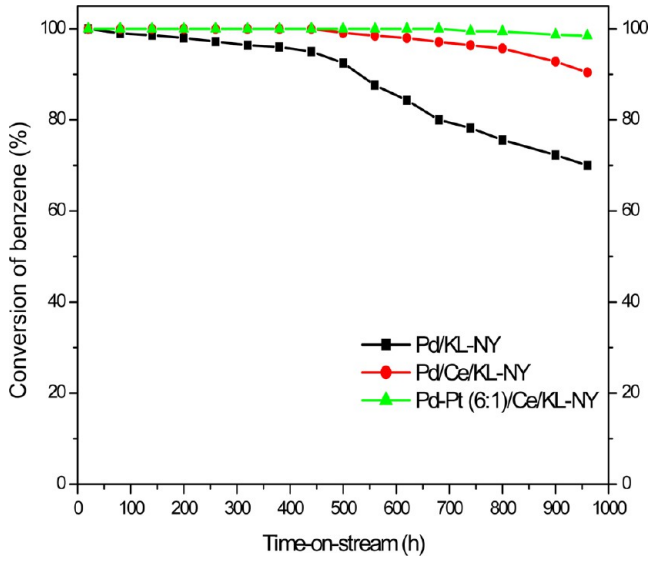

Figure 7. Evolution of benzene conversion as a function of the time-on-stream for the catalysts (space velocity: 20 000 h^{-1}; benzene: 1000 ppm; reaction temperature: 320 °C).

Ce/KL-NY catalysts between 0 and 300 °C. Blank experiments were performed using bare supports under the same conditions, and no H_2 consumption was observed. Also in Figure 8a the Pd/KL-NY and Pd/Ce/KL-NY catalysts displayed two positive peaks in the range of 0−150 °C, while the Pd−Pt (6:1)/Ce/KL-NY catalyst exhibited three peaks. The two positive peaks between 50 and 150 °C can be attributed to the two-step reduction of PdO,[52−54] which can be explained as below:

$$2PdO + H_2 \rightarrow Pd_2O + H_2O$$

$$Pd_2O + H_2 \rightarrow 2Pd + H_2O$$

For the Pd−Pt (6:1)/Ce/KL-NY catalyst, the reduction peak at 21.1 °C was attributed to the PtO_x reduction. Compared to Pd/KL-NY, it is easier to reduce Pd/Ce/KL-NY, as evidenced in the profile. The lower temperature peaks may be caused by the hydrogen consumption by PdO_x of smaller crystal sizes and higher dispersion on the KL-NY surface. Because of the addition of Pt into Pd/Ce/KL-NY, the peaks systematically shifted to lower temperatures, indicating that Pd oxides with smaller crystal sizes and higher dispersion were easier to reduce and that Pt and Ce can improve the redox property of Pd oxides. Thus, because of the interaction between the three oxides, Pd oxides were easier to reduce, which increased the lattice oxygen liability and promoted the oxidation activity. For benzene oxidation, the reduction temperatures of PdO in the catalysts were in good agreement with catalytic activities mentioned before and are ordered as follows: Pd−Pt (6:1)/Ce/

Table 2. Summary of Pd−Pt Catalysts that Are Known for Benzene Oxidation

	reaction conditions			
catalysts	Pd−Pt (wt %)	GHSV (h^{-1})	benzene (ppm)	T_{90} (°C)
$Pd/V_2O_5/Al_2O_3$[47]	0.80	30 000	482	270
Pd/ZSM-5[48]	0.27	20 000	1000	244
Pd−Pt/γ-Al_2O_3[49]	2.0−0.3	15 000	1000	225
Pd/SiO_2[50]	1.55	800	2550	197
Pd/Ce-Lap[51]	0.30	20 000	1050	250
Pd−Pt(6:1)/Ce/KL-NY [our work]	0.17−0.03	20 000	1000	205

dx.doi.org/10.1021/am500138q | ACS Appl. Mater. Interfaces 2014, 6, 11988−11996

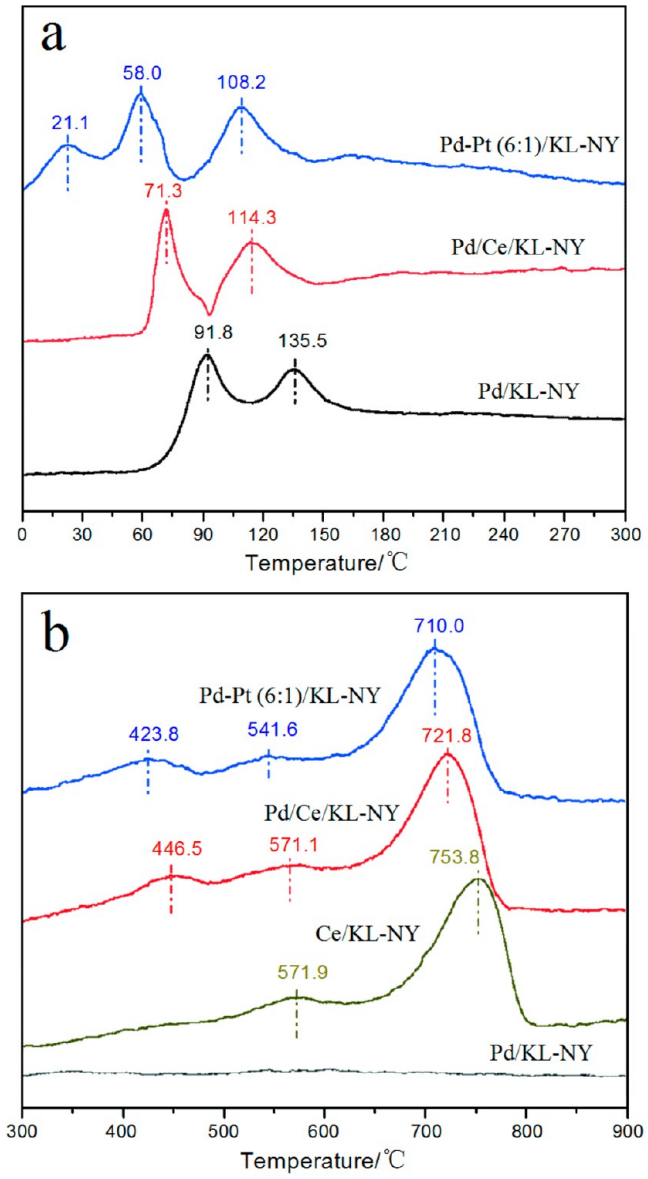

Figure 8. H_2-TPR profiles of the catalysts: (a) 0–300 °C; (b) 300–900 °C.

KL-NY < Pd/Ce/KL-NY < Pd/KL-NY. That is, PdO was more active at lower reduction temperatures, resulting in higher oxidation activity.

Figure 8b shows the H_2-TPR profiles of the catalysts between 300 and 900 °C. Similar to the reported results, the TPR profile of Ce/KL-NY showed two reduction peaks at 571.9 and 753.8 °C.[55,56] These two peaks were attributed to the reduction of surface and bulk lattice oxygen, respectively. After the addition of Pd and Pt, the two peaks systematically shifted to lower temperatures because the addition of Pd and Pt improved the oxidation properties of ceria. Furthermore, the peak attributed to the surface oxygen reduction was split into two peaks; thus, the addition of a small amount of precious metals promoted the dispersion of ceria on the KL-NY support.

In summary, adding Ce and Pt enhanced the oxidation properties of Pd catalysts, and the interactions between precious metals and ceria improved the dispersion and oxidation properties of ceria. These results are consistent with the observed catalytic activities for the complete oxidation of benzene.

CONCLUSION

In this paper, a series of KL-NY-based Pd catalysts with and without rare earth metals and Pt were obtained by the impregnation method. The studied additives greatly affected the activity of Pd/KL-NY for benzene deep combustion. Pt–Pd bimetallic catalysts were superior to the monometallic Pd catalysts, and the addition of rare earth metals (especially Ce) greatly enhanced the activity of Pd. Pd–Pt (6:1) catalysts presented the greatest activity among Pd–Pt bimetallic catalysts, and the temperature of the complete conversion of benzene was approximately 230 °C. And the Pd–Pt (6:1)/Ce/KL-NY catalyst maintained the 100% benzene conversion for 960 h. The catalysts have a framework-confined micro-mesoporous composite structure, and the mesoporous system was successfully replicated by the metal oxide and presented an ordered framework. Adding Ce and Pt enhanced the oxidation properties of Pd catalysts, and the most important factors in maintaining activity and stability were the high dispersion of PdO and CeO_2 on KL-NY, the optimal ratio of Pt and Pd and the strong interaction between ceria and precious metals.

AUTHOR INFORMATION

Corresponding Authors

*E-mail: sfzuo@usx.edu.cn. Phone: +86-575-88341832. Fax: +86-575-88341832.

*E-mail: qichenze@usx.edu.cn.

Notes

The authors declare no competing financial interest.

ACKNOWLEDGMENTS

The support from the Nature Science Foundation of China (No. 21203124) and the Foundation of Science and Technology of Shaoxing Bureau (No. 2012B70023) are gratefully acknowledged and appreciated.

REFERENCES

(1) Everaert, K.; Baeyens, J. Catalytic Combustion of Volatile Organic Compounds. *J. Hazard. Mater.* **2004**, *109*, 113–139.

(2) Aguero, F. N.; Barbero, B. P.; Gambaro, L.; Cadús, L. E. Catalytic Combustion of Volatile Organic Compounds in Binary Mixtures over $MnOx/Al_2O_3$ catalyst. *Appl. Catal., B* **2009**, *1–2*, 108–112.

(3) Zuo, S. F.; Huang, Q. Q.; Li, J.; Zhou, R. X. Promoting Effect of Ce Added to Metal Oxide Supported on Al Pillared Clays for Deep Benzene Oxidation. *Appl. Catal., B* **2009**, *1–2*, 204–209.

(4) Ojala, S.; Pitkaaho, S.; Laitinen, T.; Niskala Koivikko, N.; Brahmi, R.; Gaalova, J.; Matejova, L.; Kucherov, A.; Paivarinta, S.; Hirschmann, C.; Nevanpera, T.; Riihimaki, M.; Pirila, M.; Keiski, R. L. Catalysis in VOC Abatement. *Top. Catal.* **2011**, *54*, 1224–1256.

(5) Spivey, J. J. Complete Catalytic Oxidation of Volatile Organics. *Ind. Engine. Chem. Res.* **1987**, *26*, 2165–2180.

(6) Papaefthimiou, P.; Ioannides, T.; Verykios, X. E. Combustion of Non-Halogenated Volatile Organic Compounds over Group VIII Metal Catalysts. *Appl. Catal., B* **1997**, *13*, 175–184.

(7) Liotta, L. F.; Ousmane, M.; Di Carlo, G.; Pantaleo, G.; Deganello, G.; Marcì, G.; Retailleau, L.; Giroir-Fendler, A. Total Oxidation of Propene at Low Temperature over Co_3O_4–CeO_2 Mixed Oxides: Role of Surface Oxygen Vacancies and Bulk Oxygen Mobility in the Catalytic Activity. *Appl. Catal., A* **2008**, *347*, 81–88.

(8) Liotta, L. F.; Ousmane, M.; Di Carlo, G.; Pantaleo, G.; Deganello, G.; Boreave, A.; Giroir-Fendler, A. Catalytic Removal of Toluene over

Co_3O_4-CeO_2 Mixed Oxide Catalysts: Comparison with Pt/Al_2O_3. *Catal. Lett.* **2009**, *127*, 270−276.
(9) Zuo, S. F.; Liu, F. J.; Zhou, R. X.; Qi, C. Z. Adsorption/Desorption and Catalytic Oxidation of VOCs on Montmorillonite and Pillared Clays. *Catal. Commun.* **2012**, *22*, 1−5.
(10) Heck, R. M.; Farrauto, R. J. *Catalytic Pollution Control,* 2nd ed.; Wiley-Interscience: New York, 2002.
(11) Carballo, L. M.; Wolf, E. E. Crystallite Size Effects during the Catalytic Oxidation of Propylene on $Pt/\gamma-Al_2O_3$. *J. Catal.* **1978**, *53*, 366−373.
(12) Paulis, M.; Peyrard, H.; Montes, M. Influence of Chlorine on the Activity and Stability of Pt/Al_2O_3 Catalysts in the Complete Oxidation of Toluene. *J. Catal.* **2001**, *199*, 30−40.
(13) Cant, N. W.; Angove, D. E.; Patterson, J. M. The Effects of Residual Chlorine on the Behaviour of Platinum Group Metals for Oxidation of Different Hydrocarbons. *Catal. Today* **1998**, *44*, 93−99.
(14) Radic, N.; Grbic, B.; Terlecki-Baricevic, A. Kinetics of Deep Oxidation of *n*-Hexane and Toluene over Pt/Al_2O_3 Catalysts: Platinum Crystallite Size Effect. *Appl. Catal., B* **2004**, *50*, 153−159.
(15) Cant, N. W.; Hall, W. K. Catalytic Oxidation: II. Silica Supported Noble Metals for the Oxidation of Ethylene and Propylene. *J. Catal.* **1970**, *16*, 220−231.
(16) Bénard, S.; Ousmane, M.; Retailleau, L.; Boreave, A.; Vernoux, P.; Giroir-Fendler, A. Catalytic Removal of Propene and Toluene in Air over Noble Metal Catalyst. *Can. J. Civ. Eng.* **2009**, *36*, 1935−1945.
(17) Völter, J.; Leitz, G.; Spindler, H.; Lieske, H. Role of Metallic and Oxidic Platinum in the Catalytic Combustion of *n*-Heptane. *J. Catal.* **1987**, *104*, 375−380.
(18) Hermia, J.; Vigneron, S. Catalytic Incineration for Odour Abatement and VOC Destruction, Catalytic Incineration for Odour Abatement and VOC Destruction. *Catal. Today* **1993**, *17*, 349−358.
(19) Lyubovsky, M.; Pfefferle, L. Complete Methane Oxidation over Pd Catalyst Supported on α-alumina. Influence of Temperature and Oxygen Pressure on the Catalyst Activity. *Catal. Today* **1999**, *47*, 29−44.
(20) Yashima, M.; Falk, L.; Palmqvist, A.; Holmberg, K. Structure and Catalytic Properties of Nanosized Alumina Supported Platinum and Palladium Particles Synthesized by Reaction in Microemulsion. *J. Colloid Interface Sci.* **2003**, *268*, 348−356.
(21) Ponec, V. Alloy Catalysts: The Concepts. *Appl. Catal., A* **2001**, *222*, 31−45.
(22) Pawelec, B.; Mariscal, R.; Navarro, R. M.; van Bokhorst, S.; Rojas, S.; Fierro, J. Hydrogenation of Aromatics over Supported Pt−Pd Catalysts. *Appl. Catal., A* **2002**, *225*, 223−237.
(23) Liu, H.; Ma, L.; Shao, S.; Li, Z.; Wang, A.; Huang, Y.; Zhang, T. Preferential CO Oxidation on Ce-Promoted $Pt/\gamma-Al_2O_3$ Catalysts under H_2-Rich Atmosphere. *Chin. J. Catal.* **2007**, *28*, 1077−1082.
(24) Yu, D. Q.; Liu, Y.; Wu, Z. B. Low-Temperature Catalytic Oxidation of Toluene over Mesoporous MnO_x-CeO_2/TiO_2 Prepared by Sol−Gel Method. *Catal. Commun.* **2010**, *11*, 788−791.
(25) Zuo, S. F.; Du, Y. J.; Liu, F. J.; Han, D.; Qi, C. Z. Influence of Ceria Promoter on Shell-powder-supported Pd Catalyst for the Complete Oxidation of Benzene. *Appl. Catal. A: Gen.* **2013**, *31*, 65−70.
(26) Djinovic, P.; Levec, J.; Pintar, A. Effect of Structural and Acidity/Basicity Changes of $CuO-CeO_2$ Catalysts on Their Activity for Water−Gas Shift Reaction. *Catal. Today* **2008**, *138*, 222−227.
(27) Huang, X. S.; Sun, H.; Wang, L. C.; Liu, Y. M.; Fan, K. N.; Cao, Y. Morphology Effects of Nanoscale Ceria on the Activity of Au/CeO_2 Catalysts for Low-Temperature CO Oxidation. *Appl. Catal., B* **2009**, *90*, 224−232.
(28) Andreeva, D.; Nedyalkova, R.; Ilieva, L.; Abrashev, M. V. Nanosize Gold-Ceria Catalysts Promoted by Vanadia for Complete Benzene Oxidation. *Appl. Catal., A* **2003**, *246*, 29−38.
(29) Bernal, S.; Blanco, G.; Pintado, J. M.; Rodríguez-Izquierdo, J. M.; Yeste, M. P. An Alternative Way of Reporting on the Redox Behaviour of Ceria-Based Catalytic Materials: Temperature-Chemical Environment−Oxidation State Diagrams. *Catal. Commun.* **2005**, *6*, 582−585.
(30) Ramírez-López, R.; Elizalde-Martinez, I.; Balderas-Tapia, L. Complete Catalytic Oxidation of Methane over $Pd/CeO_2-Al_2O_3$: The Influence of Different Ceria Loading. *Catal. Today* **2010**, *150*, 358−362.
(31) Zuo, S. F.; Qi, C. Z. Modification of Co/Al_2O_3 with Pd and Ce and Their Effects on Benzene Oxidation. *Catal. Commun.* **2011**, *15*, 74−77.
(32) Taylor, K. C. Nitric Oxide Catalysis in Automotive Exhaust Systems. *Catal. Rev. Sci. Eng.* **1993**, *35* (4), 457−481.
(33) Hosseini, M.; Barakat, T.; Cousin, R.; Aboukaïs, A.; Su, B.-L.; De Weireld, G.; Siffert, S. Catalytic Performance of Core−Shell and Alloy Pd−Au Nanoparticles for Total Oxidation of VOC: The Effect of Metal Deposition. *Appl. Catal., B* **2012**, *111−112*, 218−224.
(34) Zhao, W.; Liu, Y. H.; Wang, L.; Chu, J. L.; Qu, J. K.; Hao, Z. P.; Qi, T. Catalytic Combustion of Benzene on the Pd/Nanosize Al-HMS. *Microporous Mesoporous Mater.* **2011**, *138*, 215−220.
(35) Tsoncheva, T.; Ivanova, L.; Rosenholm, J.; Linden, M. Cobalt Oxide Species Supported on SBA-15, KIT-5 and KIT-6 Mesoporous Silicas for Ethyl Acetate Total Oxidation. *Appl. Catal., B* **2009**, *89*, 365−374.
(36) Kim, K. J.; Ahn, H. G. Complete Oxidation of Toluene over Bimetallic Pt−Au Catalysts Supported on ZnO/Al_2O_3. *Appl. Catal., B* **2009**, *91*, 308−318.
(37) Venezia, A. M.; Di Carlo, G.; Pantaleo, G.; Liotta, L. F.; Melaet, G.; Kruse, N. Oxidation of CH_4 over Pd Supported on TiO_2-Doped SiO_2: Effect of Ti(IV) Loading and Influence of SO_2. *Appl. Catal., B* **2009**, *88*, 430−437.
(38) Aguero, F. N.; Barbero, B. P.; Gambaro, L.; Cadus, L. E. Catalytic Combustion of Volatile Organic Compounds in Binary Mixtures over $MnOx/Al_2O_3$ Catalyst. *Appl. Catal., B* **2009**, *91*, 108−112.
(39) Murgich, J.; Rodriguez, M. J.; Izquierdo, A.; Carbognani, L.; Rogel, E. Interatomic Interactions in the Adsorption of Asphaltenes and Resins on Kaolinite Calculated by Molecular Dynamics. *Energy Fuels* **1998**, *12*, 339−343.
(40) Duin van, A. C.; Larter, S. R. Molecular Dynamics Investigation into the Adsorption of Organic Compounds on Kaolinite Surfaces. *Org. Geochem.* **2001**, *32*, 143−150.
(41) Liu, H.; Zhao, H.; Gao, X.; Ma, J. A Novel FCC Catalyst Synthesized via in Situ Overgrowth of NaY Zeolite on Kaolin Microspheres for Maximizing Propylene Yield. *Catal. Today* **2007**, *125*, 163−168.
(42) Feng, H.; Li, C. Y.; Shan, H. H. In Situ Synthesis and Catalytic Activity of ZSM-5 Zeolite. *Appl. Clay Sci.* **2009**, *42*, 439−445.
(43) Liu, H.; Ma, J.; Gao, X. Characterization and Evaluation of a Novel Resid FCC Catalyst Based on in Situ Synthesis on Kaolin Microspheres. *Catal. Lett.* **2006**, *110*, 229−234.
(44) Liu, H.; Bao, X.; Wei, W.; Shi, G. Synthesis and Characterization of Kaolin/NaY/MCM-41 Composites. *Microporous Mesoporous Mater.* **2003**, *66*, 117−125.
(45) Zuo, S. F.; Liu, F. J.; Tong, J.; Qi, C. Z. Complete Oxidation of Benzene with Cobalt Oxide and Ceria Using the Mesoporous Support SBA-16. *Appl. Catal., B* **2013**, *467*, 1−6.
(46) Zuo, S. F.; Huang, Q. Q.; Zhou, R. X. Al/Ce Pillared Clays with High Surface Area and Large Pore: Synthesis, Characterization and Supported Palladium Catalysts for Deep Oxidation of Benzene. *Catal. Today* **2008**, *15*, 88−93.
(47) Ferreira, R. S. G.; de Oliveira, P. G. P.; Noronha, F. B. Characterization and Catalytic Activity of $Pd/V_2O_5/Al_2O_3$ Catalysts on Benzene Total Oxidation. *Appl. Catal., B* **2004**, *50*, 243−249.
(48) He, C.; Li, J. J.; Li, P.; Cheng, J.; Hao, Z. P.; Xu, Z. P. Comprehensive Investigation of Pd/ZSM-5/MCM-48 Composite Catalysts with Enhanced Activity and Stability for Benzene Oxidation. *Appl. Catal., B* **2010**, *96*, 466−475.
(49) Kim, H. S.; Kim, T. W.; Koh, H. L.; Lee, S. H.; Min, B. R. Complete Benzene Oxidation over Pt−Pd Bimetal Catalyst Supported on γ-Alumina: Influence of Pt−Pd Ratio on the Catalytic Activity. *Appl. Catal., A* **2005**, *280*, 125−131.

(50) Lambert, S.; Cellier, C.; Gaigneaux, E. M.; Pirard, J.-P.; Heinrichs, B. Ag/SiO_2, Cu/SiO_2, and Pd/SiO_2 Cogelled Xerogel Catalysts for Benzene Combustion: Relationships between Operating Synthesis Variables and Catalytic Activity. *Catal. Commun.* **2007**, *8*, 1244−1248.
(51) Li, J. J.; Liang, Z.; Hao, Z. P.; Xu, X. Y.; Zhuang, Y. H. Pillared Laponite Clays-Supported Palladium Catalysts for the Complete Oxidation of Benzene. *J. Mol. Catal. A: Chem.* **2005**, *225*, 173−179.
(52) Ngamsom, B.; Bogdanchikova, N.; Borja, M. A.; Praserthdam, P. Characterisations of $Pd−Ag/Al_2O_3$ Catalysts for Selective Acetylene Hydrogenation: Effect of Pretreatment with NO and N_2O. *Catal. Commun.* **2004**, *5*, 243−248.
(53) Fuentes, S.; Bogdanchikova, N.; Avalos-Borja, M.; Boronin, A.; Faras, M. H.; Daz, G.; Cortes, A. G.; Barrera, A. Structural and Catalytic Properties of $Pd/Al_2O_3−La_2O_3$ Catalysts. *Catal. Today* **2000**, *55*, 301−309.
(54) Barrera, A.; Viniegra, M.; Bosch, P.; Lara, V. H.; Fuentes, S. $Pd/Al_2O_3−La_2O_3$ Catalysts Prepared by Sol−Gel: Characterization and Catalytic Activity in the NO Reduction by H_2. *Appl. Catal., B* **2001**, *34*, 97−111.
(55) Yao, H. C.; Yu Yao, Y. F. Ceria in Automotive Exhaust Catalysts: I. Oxygen Storage. *J. Catal.* **1984**, *86*, 254−265.
(56) Jobbágy, M.; Mariño, F.; Schönbrod, B.; Baronetti, G.; Laborde, M. Synthesis of Copper-Promoted CeO_2 Catalysts. *Chem. Mater.* **2006**, *18*, 1945−1950.